

# Heat Transfer Analysis of Modified Solar Collector Plate with Mini-Channel

**Zainab H. Naji1**

*Mechanical Engineering Department, University of Technology, Baghdad, Iraq*

[dr\\_alnaji\\_z@yahoo.com](mailto:dr_alnaji_z@yahoo.com)

**Mohammed Fowzi M.**

*Mechanical Engineering Department, University of Technology, Baghdad, Iraq*

[mohammed2007msc@yahoo.com](mailto:mohammed2007msc@yahoo.com)

**Maryam Ali A. Ameer**

*Mechanical Engineering Department, University of Technology, Baghdad, Iraq*

[mscmariamali22294@gmail.com](mailto:mscmariamali22294@gmail.com)

Submission date:- 23/1/2018

Acceptance date:- 6/3/2018

Publication date:- 26/7/2018

## Abstract

In this paper, experimental and numerical analyses have been executed to investigate the thermal performance of modified design of mini-channel plate solar collector. For the application of mini-channel heat exchangers, it is necessary to have perfect design tools for predicting the pressure drop and heat transfer. A numerical model combining solar radiation with convective heat transfer to the absorber plate based on mini-channel has been developed. Reynolds number ranged from 70 to 300 at the fluid flow rate ranged from 4.6 L/h to 18.35 L/h is used for experimental investigation at fluid inlet temperature (20°C); the working fluid is propylene glycol. The mini channel solar collector performance is evaluated in terms of heat transfer coefficient, Nusselt number, friction factor, and pumping power. The result revealed that when there is an increase in the mass flow rate of flowing fluid, the convective heat transfer coefficient is increased, while the friction factor is decreased.

**Keywords:** Flat plate, Mini-channel, Solar collector, Heat transfer coefficient.

## Nomenclature

Symbol	Title	Unit
$A_c$	Cross sectional area of mini-channel	(m <sup>2</sup> )
$A_{ch}$	Channel heating surface area	(m <sup>2</sup> )
$b$	Time increment	(s)
$D_h$	Hydraulic diameter	(mm)
$cp$	Specific heat capacity	(KJ/Kg K )
$H$	Channel height or thickness	(mm)
$h$	Heat transfer coefficient	(w/m <sup>2</sup> .k)
$I$	Hourly solar radiation	(J)
$I_b$	Beam hourly solar radiation	(J)
$I_d$	Direct hourly solar radiation	(J)
$I_T$	Total Hourly solar radiation	(J)

<b>k</b>	<b>Thermal conductivity</b>	<b>(w/m.k)</b>
<b>L</b>	<b>Channel length</b>	<b>(mm)</b>
<b>m•</b>	<b>Mass flow rate</b>	<b>(kg/s)</b>
<b>N<sub>g</sub></b>	<b>Number of glass cover</b>	
<b>N</b>	<b>Number of days in the year</b>	
<b>Nu</b>	<b>Nusselt number</b>	
<b>P</b>	<b>Pitch</b>	<b>(mm)</b>
<b>Q<sub>U</sub></b>	<b>Useful energy</b>	<b>(watt)</b>
<b>Q<sub>Ud</sub></b>	<b>Daily useful energy</b>	<b>(J)</b>
<b>Q<sub>R</sub></b>	<b>Daily solar radiation</b>	<b>(J)</b>
<b>Re</b>	<b>Reynolds number</b>	
<b>R<sub>g</sub></b>	<b>The ground reflectivity</b>	
<b>T</b>	<b>Temperature</b>	<b>(c°)</b>
<b>T<sub>a</sub></b>	<b>Ambient temperature</b>	<b>(c°)</b>
<b>V•</b>	<b>volume flow rate</b>	<b>(l/h)</b>
<b>W</b>	<b>Channel width</b>	
<b>Y</b>	<b>The ratios of sky diffuse radiation on vertical surface of that on horizontal surface</b>	
<i>Greek symbols</i>		
<b>ρ</b>	<b>Density</b>	<b>(Kg/m<sup>3</sup>)</b>
<b>η</b>	<b>Collector efficiency</b>	
<b>η<sub>i</sub></b>	<b>Instantaneous efficiency</b>	
<b>ατ</b>	<b>Effective transmittance-absorptance</b>	
<b>Φ</b>	<b>Latitude angle</b>	<b>(degree)</b>
<b>Δ</b>	<b>Declination angle</b>	<b>(degree)</b>
<b>Γ</b>	<b>Surface azimuth angle</b>	<b>(degree)</b>
<b>B</b>	<b>Surface tilt angle</b>	<b>(degree)</b>
<b>ω</b>	<b>Hour angle</b>	<b>(degree)</b>
<b>Θ</b>	<b>Incidence angle</b>	<b>(degree)</b>
<b>θ<sub>2</sub></b>	<b>Reflected angle</b>	<b>(degree)</b>
<b>θ<sub>g</sub></b>	<b>Effective angle of ground reflectance</b>	
<b>θ<sub>d</sub></b>	<b>Effective angle of incidence of diffuse</b>	
<b>θ<sub>z</sub></b>	<b>Zenith angle</b>	<b>(degree)</b>
<b>α</b>	<b>Solar absorptance</b>	
<b>α<sub>s</sub></b>	<b>Solar altitude angle</b>	<b>(degree)</b>
<b>γ<sub>s</sub></b>	<b>Solar azimuth angle</b>	<b>(degree)</b>
<b>τα<sub>b</sub></b>	<b>Transmittance-absorptance for beam radiation</b>	
<b>τα<sub>d</sub></b>	<b>Transmittance-absorptance for diffuse radiation</b>	
<b>τα<sub>g</sub></b>	<b>Transmittance-absorptance for ground radiation</b>	
<b>Δp</b>	<b>Differential pressure</b>	<b>Pa</b>
<b>f</b>	<b>Fraction factor</b>	
<i>Subscripts</i>		
<b>f</b>	<b>Fluid</b>	
<b>in</b>	<b>Inlet fluid</b>	
<b>out</b>	<b>Outlet fluid</b>	

## 1. Introduction

The study of renewable energies (the near-term resurgence and source of natural resources) has become a target for many scientists and researchers because they are better than fossil fuels. Particularly, different technologies that use solar energy have been checked by different industries and universities so to evolve many ways that are cost competitive and environmentally friendly to generate power, cooling and heating, for residential and commercial uses. The thermal system of solar (such as air heaters, solar water heaters and dryers) is one of the systems in which the solar energy could be utilized. Solar water heating, specifically, flat solar heater, is widely used in most of the countries in all over the world especially in The Middle East region. Since 1891, the solar energy has been utilized to heat the water [1], and the patented Climax solar water heater was the primary commercial model. After that, a number of collector designs have been suggested, like flat plate [2], evacuated tube collectors [3], and units that need compound parabolic concentrators [4]. The small scale channels (micro or mini) have been a famous field of investigation for the previous three decades owing to their high rate of heat transfer, especially for heat exchangers. Many reviews were performed by different investigators about characteristics of flow and heat transfer in mini-channels under heat flux conditions, such as [5] and [6]. Tubes having mini-channels are categorized according to their hydraulic diameter over the range between 200  $\mu\text{m}$  and 3 mm [7]. Investigated the thermal performance of a new design of mini-channel-based solar flat-plate collector. The solar collector consists of an array of mini-channels located in the absorber plate which is covered by a single glass cover [8], studied flat plate absorbers that may pass the fluid through a tube bonded to a thermally conducting plate or achieve lower thermal resistance and pressure drop by using a flooded panel or micro-channel design. The optimum diameters were in the range (6–16) mm depending on the pumping power and (diameter/pitch) ratio [9]. Presented novel solar-thermal arrays for facades integration, based on a trapeze-shaped solar-thermal collector [10]. Solar collectors differ in performance relying on their design. Effectively, one important topic that stays a matter of intensive research is transferring the heat sun to the operating fluid. The present paper analyzes the performance of modified solar collector based on mini-channel to raise the heat-transferred quantity to the operating fluid. The characteristics of the solar collector having mini-channels are based on the absorber plate design, selective coatings, thermal insulation, tilt angle of the collector and working fluids. The present work is used adequately model the heat transfer in a new design of mini-channel collector based on solar radiation with possibility of increasing the energy efficiency of thermal process.

## 2. Experimental Work:

Solar collector based on mini-channel has been manufactured from two absorbing metal plates made of (Aluminum, alloy 6061 T6). The dimensions of each plate are (700 mm $\times$ 400 mm) with thickness of (20 mm). Computer Numerical Control (CNC) is used to drill (46 mini-channel) with square cross section area (3 mm $\times$ 3 mm), considering that the distance between the channels is (11 mm) in the top plate as shown in fig.(1). Grooves are made on the top surface of the plate to fix seven thermocouples; the distance between them is 100 mm, as shown in fig. (2). A hole is made in the top plate to show the outlet and inlet of the working fluid and two thermocouples have been used to measure the outlet and inlet temperatures of the working fluid, then the two plates are joined with screws. Now, the mini-channel is

ready for any scientific tests. The diagram of the test facility is schematically depicted in fig. (3). While the mini-channel absorbing plate is shown in fig.(4) finally, the sample is smoothly cleaned by soft silky fabric until one should almost see himself on it. The test section (i.e. solar collector based on mini-channel) composed of a temperature controlled storage tank, circulation pump, connecting pipes and fittings, measuring devices which consist of: solar radiation measurement, two flow meters; the first one used at range (1-10 L/h) and the other one used at range (1.6-16 L/h), two pressure gages to measure the pressure difference across the test section, temperature controller and thermocouples type (K).



**Figure (1): Test Mini-Channels Solar Collector.      Figure (2): Thermocouples Location at The top Plate**

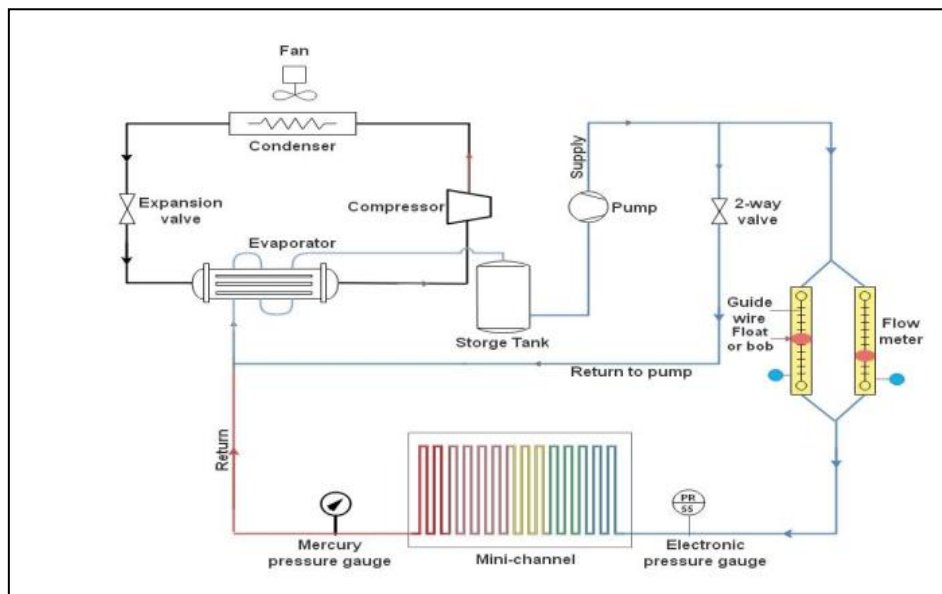


**Figure (3) Schematic Representation of Test Facility**

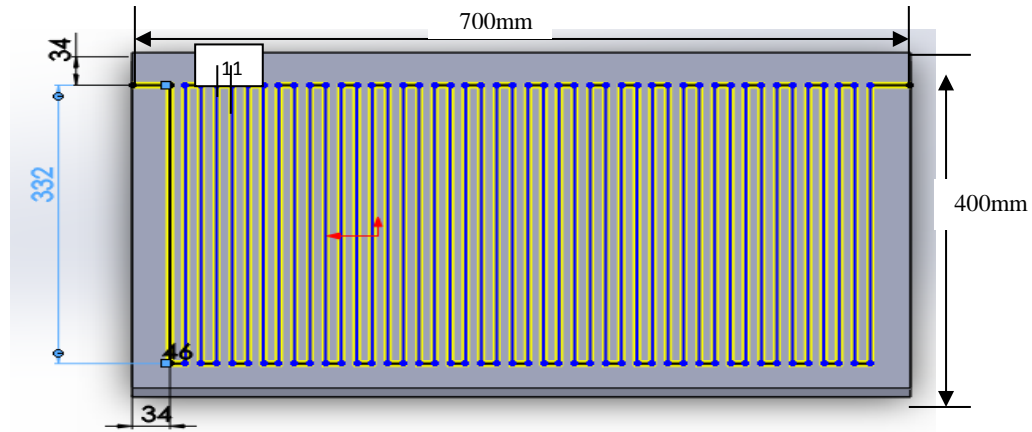


**Figure (4) Mini channel absorbing**

### A. Experimental Procedure

In this paper, study the test rig with glass cover the tests were conducted in Baghdad with southeast orientation at latitude (33.3 °) during July. The data was recorded from (8:00 Am to 6:00 Pm). Working fluids is propylene glycol was chosen in the tests with five different mass flow rates as follows: (4.6, 5.77, 7.96, 11.2 and 18.35) L/h. The mini-channel solar collector was tested under a steady-state condition. The following test procedures were considered:

1. Recording the date and time of experiment.
2. Measuring the ambient temperature.
3. Turning on cooling system, which controlled the constant temperature storage tank to a chive the desired fluid inlet temperature. In these tests, inlet temperature was considered (20°C).
4. Operating the circulating pump to adjust the flow rate to the exact desired value by gradually controlling the flow rate by using control valve and flow meter, which are constantly checked in order to get the accurate value of flow rate.
5. Measuring the solar radiation intensity, which initiates the heating at the test section.
6. Recording the inlet and outlet temperature of the working fluid and the temperatures distributed along the plate.
7. Recording the pressures across the test section.
8. Repeating the experiments every 60 minutes for 10 hours.

### B. Experimental Data Analysis

The calculations were done by conventional equations [11]. The mass flow rate is computed by measuring the volume flow rate and density of propylene glycol.

$$\dot{m} = \rho \cdot \dot{V} \quad \dots (1)$$

Hydraulic diameter was calculated by using the formula

$$D_h = \frac{4A_c}{P} \quad \dots (2)$$

Where,  $A_c$ : channel cross-sectional area,  $P$ : perimeter of channel.

For Reynolds number

$$\mathbf{Re} = \left( \frac{\rho u D_h}{\mu} \right) \quad \dots (3)$$

Where,  $\rho$  is the density of fluid,  $\mu$  is the fluid dynamic viscosity,  $u$  is the velocity of fluid, and  $D_h$  is hydraulic diameter of fluid.

Friction factor was calculated including entrance and exit loses

$$f = \frac{1}{2} \frac{D_h}{L} \frac{\Delta P}{\rho \cdot u_m^2} \quad \dots (4)$$

Where  $\Delta P$ : pressure difference that measured by a pressure transducer;  $\Delta p = p_{out} - p_{in}$

The total heat that transferred to the fluid across the test section and represented as hour useful energy for mini-channel solar collector, is given by:

$$\mathbf{Q_u} = \dot{m} \cdot C_p \cdot (\mathbf{T_{f(out)}} - \mathbf{T_{f(in)}}) \quad \dots (5)$$

Where;  $C_p$  = Specific heat capacity of propylene glycol (kJ/kg.°C) and  $(\mathbf{T_{f(out)}}$ ,  $\mathbf{T_{f(in)}}$ ) = Inlet and outlet propylene glycol temperatures (°C).

The heat flux is compute by dividing  $\mathbf{Q_u}$  by the channel heating area  $A_{ch}$

$$\mathbf{q_u} = \frac{\mathbf{Q_u}}{A_{ch}} \quad \dots (6)$$

It is assumed that the longitudinal fluid temperature in the test section is linearly varying, it is calculated as follows:

$$\mathbf{T_f(x)} = \mathbf{T_{f,i}} + (\mathbf{T_{f,o}} - \mathbf{T_{f,i}}) \cdot \frac{x}{L} \quad \dots (7)$$

The coefficient of local heat transfer can be defined as:

$$\mathbf{h(x)} = \frac{q}{[T_p(x) - T_f(x)]} \quad \dots (8)$$

Where,  $T_p(x)$  are the measurements of temperature along the plate by thermocouples.

The local Nusselt number can be defined as:

$$\mathbf{Nu(x)} = \frac{\mathbf{h(x) \cdot D_h}}{k_f(x)} \quad \dots (9)$$

The average Nusselt number can be computed by using the average value of seven readings of local Nusselt number for each experiment.

$$\mathbf{Nu_m} = \frac{1}{7} \sum \mathbf{Nu(x)} \quad \dots (10)$$

Trapezoidal rule has been used to calculate the daily useful energy ( $\mathbf{Q_u}$ ) for solar collector [12].

$$\mathbf{Q_{ud}} = \sum_{ti}^{tf} \mathbf{qt} = \mathbf{b} \left[ \frac{\mathbf{Q_{u1}}}{2} + \mathbf{Q_{u2}} + \mathbf{Q_{u3}} + \dots + \frac{\mathbf{Q_{un}}}{2} \right] \quad \dots (11)$$

Where,  $b$  is time increments=1800 second, and  $qt$  is useful energy at that time.

The daily solar radiation for mini-channel solar collector as:

$$Q_R = A_C * b * \left[ \frac{It_1}{2} + It_2 + It_3 + \dots + \frac{It_N}{2} \right] \quad \dots (12)$$

Where, **AC**: Collector area (m<sup>2</sup>).

The instantaneous collector efficiency can be calculated using the following equation:-

$$\eta_i = Q_U / (A_C \cdot I_T) \quad \dots (13)$$

To calculate the daily efficiency for mini-channel solar collector:

$$\eta = Q_{Ud} / Q_R \quad \dots (14)$$

### 3. Numerical Analysis

#### a) Problem Statement and Assumptions

The geometry in the present work as depicted in fig. (4) Is a uniform aluminum rectangular plate (400 mm×700 mm×40 mm) with serpentine-shape channel with sectional area (3 mm×3 mm) and the length of the channel is 15767 mm. The working fluid is propylene glycol flows through it with flow rates range (4.6L/h to 18.35 L/h). The obtained numerical results showed that such design would enhance the heat transfer from the riser pipes walls to the liquid and thus would yield the hot propylene glycol manufacturing capacity of the solar collector.

In the analysis, laminar flow, incompressible flow, steady state, uniform heat flux, and three-dimensional are assumed.

#### b) Numerical Model

For analyzing the field of flow in the flat plate with serpentine shape mini-channel solar collector subjected to heat flux, equations of continuity, energy and momentum are required to be solved. The calculated range is meshed with control volumes established about every grid by employing Solid work (preprocessor for FLUENT). The process of numerical simulation was conducted through a steady-state implicit pressure based solver built in commercial FLUENT software “version 16.1”. For the steady incompressible flow, solutions of the governing partial differential equations for energy and mass momentum are obtained. The coupling of velocity-pressure was affected using the semi implicit method for pressure-linked equations (SIMPLE) algorithm evolved by Patankar [13]. Schemes of the second order upwind were selected for the solution ones. A laminar flow state was utilized, and generations of three- dimensional mesh were established.

The governing partial differential equations are as follows:

Continuity:

$$\nabla(\rho V) = 0 \quad \dots(15)$$

Momentum equation

$$\frac{\partial}{\partial x_i} (\rho U_i U_j) = \frac{\partial \rho}{\partial x_i} + \frac{\partial}{\partial x_j} \left[ \mu \left( \frac{\partial U_i}{\partial x_j} + \frac{\partial U_j}{\partial x_i} \right) - \overline{\rho U_i U_j} \right] \quad \dots(16)$$

Energy equation

$$\frac{\partial}{\partial x_j} (\rho U_i T) = \frac{\partial}{\partial x_j} \left[ \frac{\mu}{Pr} \frac{\partial T}{\partial x_j} - \overline{\rho U_i T} \right] \quad \dots(17)$$

### c) Boundary Conditions and the Operating Parameters

Based on the working fluid flow rate, the boundary condition of inlet is expressed as the velocity inlet condition (0.14 m/s, 0.178 m/s, 0.246 m/s, 0.3395 m/s, 0.565 m/s). The inlet temperature of fluid (20°C) and all data are supplied from the experiments. The boundary condition of outflow is used at the outlet. Wall The boundary of the wall are applied to limit the solid and fluid zones. At the wall, in the models of viscous flow, the components of velocity are set to zero according to the states of no-slip and impermeability that present there. The propylene glycol - absorber plate interface is described as a wall having a coupled state for affecting the conjugate heat transfer from the absorber channel to the propylene glycol. Variable heat flux tantamount to solar radiation is used at the absorber plate top surface (Table (1)). The absorber tube outer surface and the absorber plate bottom and side surfaces are described as a wall having a zero heat flux state for affecting the insulated conditions. For both absorber plates, the used material is aluminum. The analysis used input factors are listed in Table (2). Information on the solar energy that absorbed by the collector absorber plate is needed to predict the performance of collector. The incident of solar energy on an inclined surface can be determined by [14]. Through the present investigation, the absorbed energy from the absorber plate will be imposed as a uniform heat flux using MATLAB to find the solar collector performance based on a mini channel.

### Calculations of Solar Radiation

Calculations of solar radiation includes finding the beam and the diffuse radiation.

$$I_T = I_b + I_d \quad \dots (18)$$

The beam radiation component ( $I_b$ ) on a collector surface can be determined for a specific angle of incident by the following relationship (ASHRAE 2005) [11]:

$$I_b = I_{dn} * \cos\theta \dots (19), I_{dn} = \left( \frac{A}{\exp\left(\frac{B}{\sin\alpha_s}\right)} \right) \quad \dots (19)$$

Where:

$$\sin \alpha_s = \cos\phi * \cos\delta * \cos\omega + \sin\phi * \sin\delta \quad \dots (20)$$

(A) and (B) values were computed by equations (21) and (22) [13].

$$A = 1158 * (1 + 0.066 * (\cos(Z))) \quad \dots (21)$$

$$B = 0.175 * (1 - 0.2 * (\cos(Z1))) - 0.004 * (1 - (\cos(Z2))) \quad \dots (22)$$

$$\text{Where, } Z = \left( 360 * \frac{n}{370} \right) = 0.93 * n, Z2 = 1.86 * n \quad \dots (23)$$

### Calculation of Diffuse Radiation

The diffuse radiation component ( $I_d$ ) of solar radiation can be computed as follows [13]:

The diffuse radiation for a vertical or a tilted surface is

$$I_{ds} = Y.C.I_{dn} \quad \dots (24)$$



Where,  $Y$  is the ratio of sky diffuses radiation on the vertical surface to that on the horizontal one.

$C$ : is a dimensionless value representing the diffuse average ratio to the normal beam radiation.

$$Y = 0.55 + 0.437 * \cos\theta + 0.313 * \cos\theta^2 \quad \dots(25)$$

$$C = 0.0965 * (1 - 0.42 * \cos(z)) - (0.0075 * (1 - \cos(1.95 * n))) \quad \dots(26)$$

The reflected radiation of ground can be determined form the equation below: [13]

$$I_{dg} = 0.5 * r_g * I_{dn} * (C + \sin(\alpha_s)) * (1 - \cos(\beta)) \quad \dots(27)$$

Where,  $r_g$  is the reflectivity of ground equal to 0.4 [13].

$$I_d = I_{dg} + I_{ds} \quad \dots(28)$$

The collector performance prediction needs the information about the solar energy absorbed ( $S$ ) by the absorber plate of collector. The incident of solar on an inclined surface can be determined the following equation by [13]:

$$S = (I_b * R_b * \tau\alpha_b) + I_d * \tau\alpha_d * \frac{1+\cos(\beta)}{2} + r_g * \tau\alpha_g * \frac{1-\cos(\beta)}{2} \quad \dots(29)$$

Where,  $(\tau\alpha_b)$  is the transmittance - absorptance product for beam,  $(\tau\alpha_d)$  is the diffuse radiation component, and  $(\tau\alpha_g)$  is the ground-reflected radiation component. The transmission, reflection, and solar radiation absorption by the different solar collector parts are significant in finding the performance of collector. These are functions of the glass thickness ( $L$ ), material extinction coefficient ( $KL$ ), glass cover refractive index ( $n$ ), and incident solar radiation ( $IT$ ), and eventually, each value of transmittance - absorptance product for the three components of incident radiation are substituted in equation (19) to determine the net of absorbed radiation on the collector surface.

**Table (1): Heat Flux Variation with Time of Day**

Time	Heat flux				
	U= 0.14 (m/s)	U= 0.17 (m/s)	U=0.25 (m/s)	U=0.3 (m/s)	U=0.5 (m/s)
8:00 AM	277.032	277.4608	277.9146	278.3921	278.8921
9:00 AM	477.2625	478.0127	478.8096	479.6514	480.5364
10:00 AM	636.3842	637.3253	638.3235	639.3761	640.4802
11:00 AM	737.4476	738.2853	739.1675	740.0917	741.0558
12:00 PM	773.6834	774.4871	775.3158	776.1672	777.0405
1:00 PM	737.4476	738.2853	739.1675	740.0917	741.0558
2:00 PM	636.3842	637.3253	638.3235	639.3761	640.4802
3:00 PM	477.2625	478.0127	478.8096	479.6514	480.5364
4:00 PM	277.032	277.4608	277.9146	278.3921	278.8921
5:00 PM	93.9464	94.0023	94.0581	94.1134	94.1675
6:00 PM	23.8827	23.7872	23.6835	23.5715	23.4508

**Table (2): Simulation Input Parameters**

Parameter	Value
<b>Density (aluminum )</b>	2719 kg/m <sup>3</sup>
<b>Specific Heat (aluminum)</b>	871 J/kg-K
<b>Thermal Conductivity (aluminum)</b>	202.4 W/m-K
<b>Density (propylene glycol )</b>	1032 kg/m <sup>3</sup>
<b>Viscosity(propylene glycol )</b>	0.0038kg/(m.s)
<b>Specific Heat ( propylene glycol)</b>	3600 J/kg-K
<b>Thermal Conductivity ( propylene glycol)</b>	0.42W/m-K

## 4. Results and Discussion

### 1. Temperature Distribution

Different solar radiations rates were used when conducting experiments in order to understand the effects of solar radiation. Figures (5a) and (5b) depict the temperature distribution of the flat plate of absorber solar collectors, with time for fluid mass flow rates ( $\dot{m}=5.77$  L/h and at  $\dot{m}=18.35$  L/h), respectively, where (x) represents the thermocouple's location. Generally, the absorber plate temperature distributions rise progressively in the flow direction within the mini-channel. Figure (6) reveals the temperature distribution along the absorbing plate, it can be noted in this figure that the plate temperature is increased along the length of the plate for different mass flow rates. Figure (7) shows the temperature distribution of the propylene glycol within the mini-channel for different mass flow rates (4.6 L/h, 5.77 L/h, 7.96 L/h, 11.2 L/h and 18.35 L/h). The temperature of propylene glycol was raised in the flow direction within the mini-channel. The obtained results indicated that the temperature of propylene glycol at low flow rate is greater than those for other rates of mass flow. Figure (8) manifests the numerical results of temperature contours along the plate. The comparison between the experimental and theoretical results of outlet temperature of fluid, for the three various rates of mass flow, is shown in fig. (9). According to these figures, one can conclude that as the solar radiation increases, the temperature of absorber plate and the temperature difference of fluid between the inlet and outlet of channel increase. Increasing the Reynolds number (i.e. increasing in mass flow rate) decreases the temperature difference between the inlet and outlet of channel. This shows that the lower Reynolds numbers should be regarded in the laminar zone for heating uses. Also using glass cover and working fluid is propylene glycol glass cover leads to increase temperature distribution of absorber plate. The reason for this is conveniently foreseeable because of the cover thermal resistance, which causes a decrease in energy loss to the ambient, thus the heat capacity is larger.

### 2. Beneficial Energy

Figure (10) illustrates the beneficial energy of flat plate solar collectors with propylene glycol and serpentine shape mini-channel at different rates of mass flow. Obviously, the beneficial energy at high fluid mass flow rate inside mini-channel is greater than others, and percentage of increase in the beneficial energy versus mass flow rate is about 5%. Also, it can be indicated from the figure that the comprising between the beneficial energy (experimental and theoretical), and between solar

radiation (experimental and theoretical) for different mass flow rates have a well agreement.

### 3. Friction Factor

For a laminar fully developed flow, the friction factor is presented in fig. (11), as a function of Reynolds number. It can be indicated that the measuring data are set to be decreasing in friction factor with increasing Reynolds number. Figure (12) shows the deferential pressure,  $\Delta P$  versus Reynolds number, and fig. (13) depicts the differential pressure,  $\Delta P$  versus mass flow rate, it can be indicted from these two figures that  $\Delta P$  increases with increasing Reynolds number and mass flow rate, respectively.

### 4. Pumping Power

Important parameter in the Mini-channel operation is the pressure drop which relates to the working fluid pumping power required. It is the product of the pressure drop across the test section,  $\Delta P$  and volume flow rate,  $V$ . Pumping power =  $Q\Delta P$ . Where,  $Q$  is volume flow rate in  $m^3/s$ . Figure (14) shows the plot of pumping power with fluid velocity. Lower pumping power yields higher overall fluid temperatures due to the lower fluid velocities.

### 5. Heat Transfer Characteristics

Figure (15) views the heat transfer coefficient versus fluid velocity of experimental value of serpentine shape mini-channel. Obviously, coefficient of the heat transfer rises by increasing fluid velocity. Similarly, in Figure (16), a Reynolds number dependent Nusselt number can be observed. Nusselt number for thermally developing flow is increasing with increase Reynolds number.

### 5. Conclusions

This section presents the conclusions about the work of this thesis which focused on investigating the effect of heat transfer and flow field on the performance of serpentine mini-channel solar collector. The main conclusions can be listed as follows:

1. The temperature distributions of the absorber plate solar collector based on mini-channel increase gradually to the direction of flow along the mini-channel, and the working fluid outlet temperature was increased in the direction of flow inside the mini-channel for test case when increasing the solar radiation.
2. The temperature of absorber plate and working fluid increase when the solar radiation increases and mass flow rate decrease for the inlet temperatures were considered ( $20^\circ C$ ).
3. Hydraulic performance is one characteristic that influences the mini-channel design the pressure drop increases when increasing Reynolds number and fluid velocity. The increase in Reynolds number will result in lower average friction factors. Also pumping power is an important parameter in the mini-channel operation. Lower pumping power yields higher overall fluid temperatures.
4. Heat transfer coefficient can be improved by reducing the hydraulic diameter.

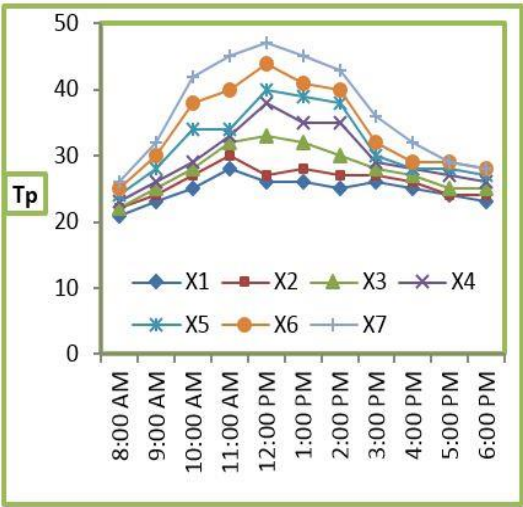


Figure (5a): Temperatures of PI ate with Time at ( $m=5.77$  L/h)

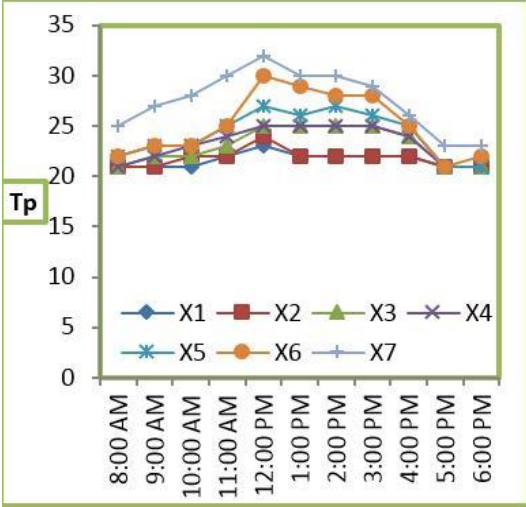


Figure: (5b) Temperatures of Plate Time at ( $m=18.35$  L/h)

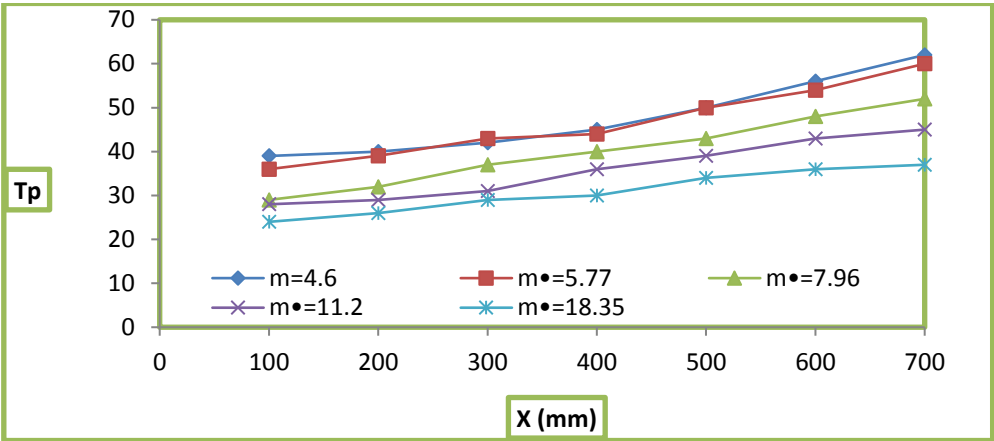


Figure: (6) Temperatures of Plate with Plate Length at (12:00 pm)

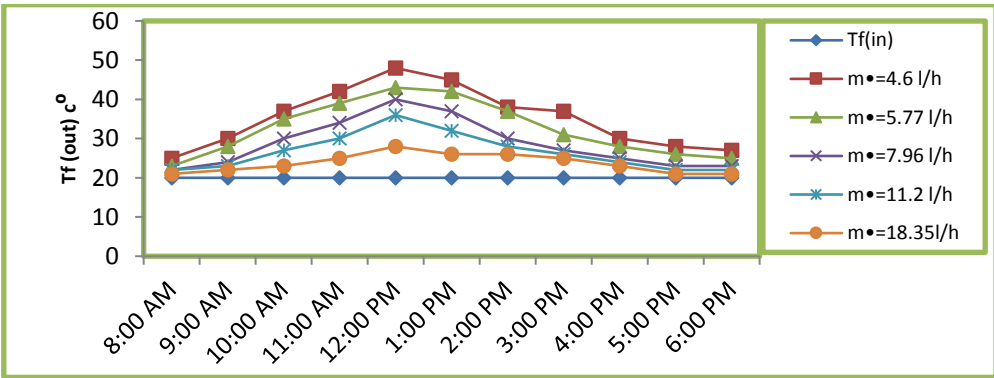


Figure (7): Temperatures of Fluid with Time.

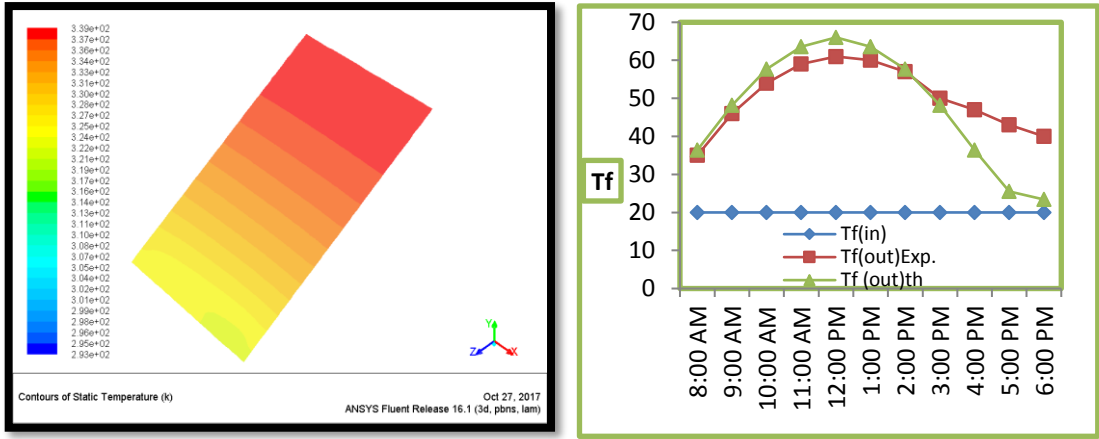
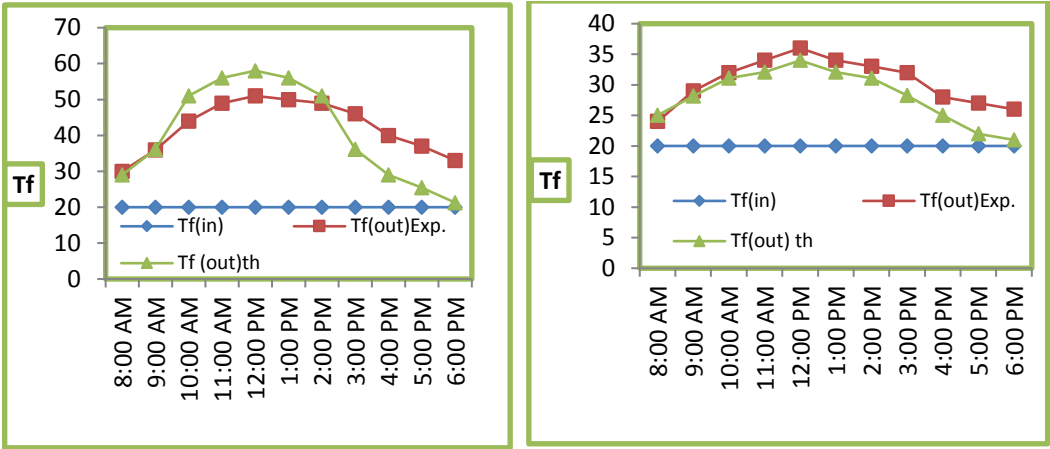


Figure (8): Temperature Contours along the Plate.

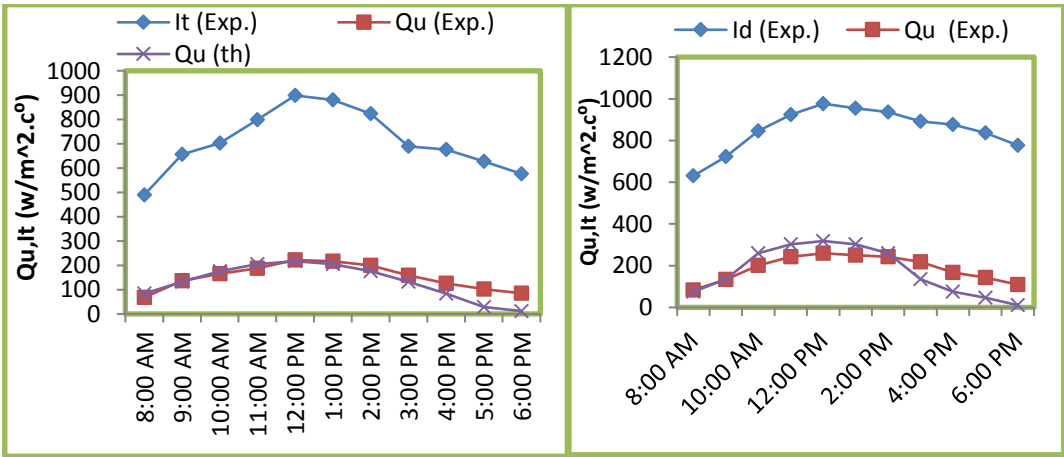
a. at ( $\dot{m}=4.6$  L/h)



b. at ( $\dot{m}=7.9$  L/h)

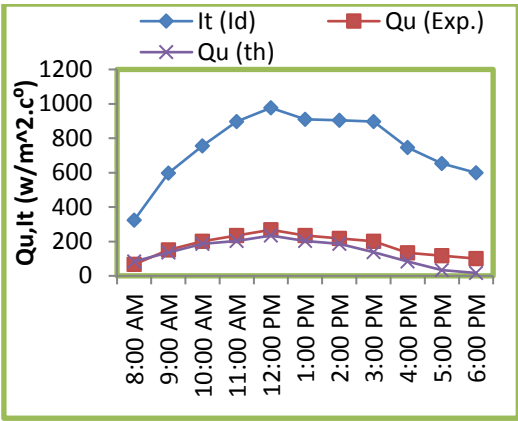
c. at ( $\dot{m}=18.3$  L/h)

Figure (9): Comparison between the Experimental and Theoretical Results of Outlet Fluid Temperature for Different Mass Flow Rates; cases (a, b, c).



a. at(5.77 L/h)

b. at(7.96 L/h)



c. at (18.3 L/h)

Figure (10): Comparisons between Useful Energy (Experimental and Theoretical), and Solar Radiation Experimental for Different Mass Flow Rates; cases (a, b, c).

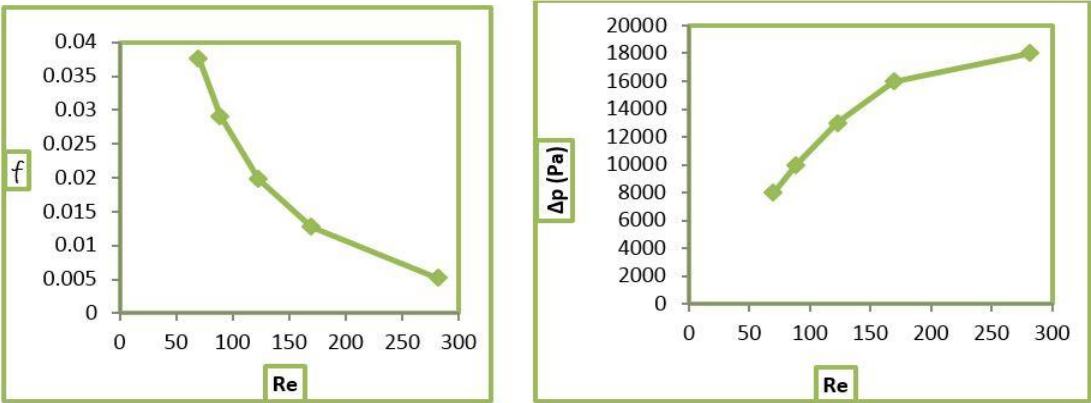


Figure (11): Friction Factor against Reynolds Number

Figure (12): Differential pressure against Reynolds Number.

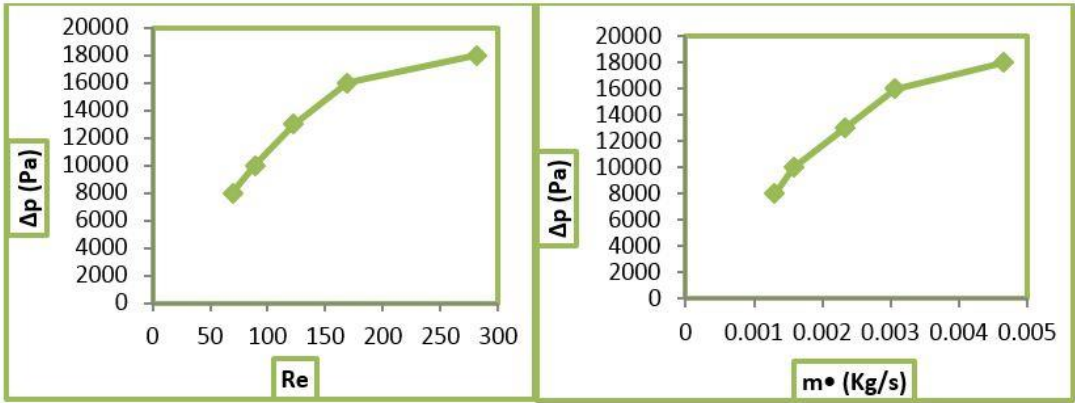


Figure (13): Differential pressure against Mass Flow rate

Figure (14): Pumping power against Fluid Velocity

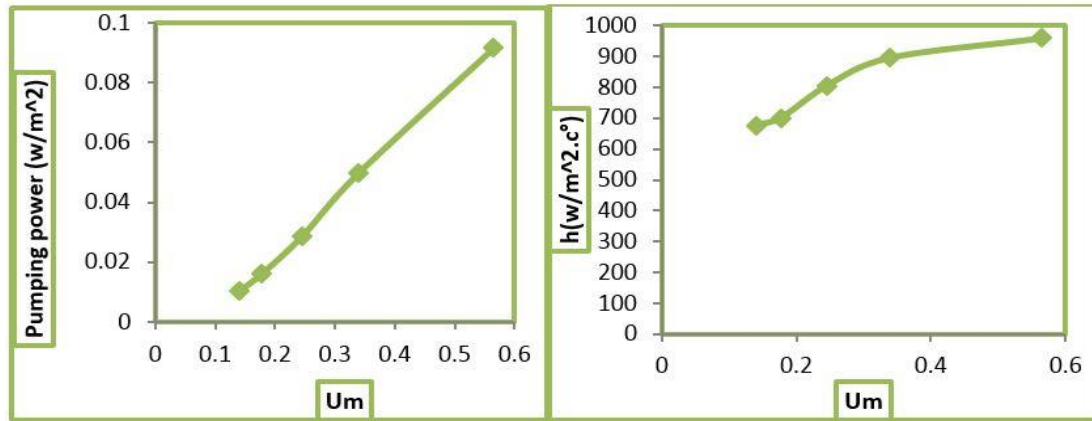


Figure (14): Pumping power against Fluid Velocity Figure (15): Heat Transfer Coefficient against Main Velocity at (12:00Pm)

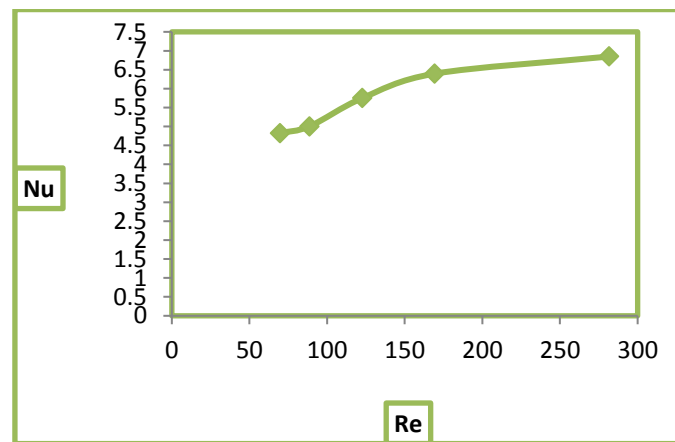


Figure (16): Nusselt Number against Reynolds Number at (12:00 Pm)

## References

- [1] Kemp C. M., "Apparatus for utilizing the sun's rays for heating water", US patent 451384, 1891.
- [2] Duffie J. A., and Beckman W. A., "Solar Engineering of Thermal Processes". John Wiley & Sons Inc., 2006.
- [3] Ayompe L., and Duffy A., "Thermal performance analysis of a solar water heating system with heat pipe evacuated tube collector using data from a field trial". Solar Energy, 90, pp. 17–28, 2013.
- [4] Rabl A., O'Gallagher J., and Winston R., "Design and test of non-evacuated solar collectors with compound parabolic concentrators". Solar Energy, 25, pp. 335–351, 1980.
- [5] Jiri Hejcik and Miroslav Jicha, "Single phase heat transfer in minichannels". EPJ Web of Conferences 20 34 67, published by EDP Sciences, 2014.
- [6] P. Dheenathayalan, K. Chandrasekaran, J. Rajasekaran, and T. Rajaprabu "Experimental Investigation of Fluid Flow and Heat Transfer in Internally Finned Minichannels". International Journal of Emerging Technology and Innovative Engineering Volume I, Issue 3, March 2015.

- [7] Steinke M. E. and Kandlikar S. G., "Single-phase heat transfer enhancement techniques in micro-channel and mini-channel flows." *Proceedings of Micro-channels and Mini-channels ASME Conference*, ICMM2004-2328, pp. 141–148, 2004.
- [8] M. Khamis Mansour "Thermal analysis of novel minichannel-based solar flat-plate collector" Vol. 60, 1, pp. 333-343, oct.2013
- [9] R.W. Moss, G. S. F. Shire, P. Henshall, P.C. Eames, F. Arya, and T. Hyde d "Optimal passage size for solar collector micro-channel and tube-on-plate absorbers", *Solar Energy* 153, pp.718–731, 2017.
- [10] Ion Visaa, Macedon Moldovana, Mihai Comsita, Mircea Neagoea, and Anca Dutaa "Facades integrated solar-thermal collectors – challenges and solutions". *Energy Procedia*, 112 pp.176 – 185, 2017.
- [11] Kakaç S, Yener Y. *Convective Heat Transfer*, Second edition CRC press, Washington, 1994.
- [12] ASHRAE, *Handbook of Fundamentals*, Atlanta: American Society of Heating, Refrigerating, and Air- Conditioning Engineers, Inc., 2005
- [13] Patankar S. V. and D. B. Spalding, "A calculation procedure for heat, mass and momentum transfer in three-dimensional parabolic flows", *International Journal of Heat Mass Transfer*, Vol. 15, p.1787, 1972.
- [14] Duffie J. A. and Beckman W. A., "Solar Engineering of Thermal Processes", Third Edition, John Wiley & Sons, Interscience, New York, 2006.



زينب حسون ناجي

قسم الهندسة الميكانيكية، الجامعة التكنولوجية، بغداد، العراق

[dr\\_alnaji\\_z@yahoo.com](mailto:dr_alnaji_z@yahoo.com)

محمد فوزي محمد

قسم الهندسة الميكانيكية، الجامعة التكنولوجية، بغداد، العراق

[mohammed2007msc@yahoo.com](mailto:mohammed2007msc@yahoo.com)

مريم علي عبد الامير

قسم الهندسة الميكانيكية، الجامعة التكنولوجية، بغداد، العراق

[mscmariyamali22294@gmail.com](mailto:mscmariyamali22294@gmail.com)

الخلاصة

الهدف من هذه الدراسة تنفيذ التحليلات العملية والعديدية للتحقيق في الأداء الحراري للوح مجمع طاقة شمسية يعمل على اساس قناة مصغرة. لتطبيق المبادلات الحرارية قناة صغيرة، فمن الضروري أن يكون أدوات تصميم مثالية لتتبع انخفاض الضغط ونقل الحرارة. النموذج الرقمي يجمع بين الإشعاع الشمسي مع نقل الحرارة الحمل إلى لوحة امتصاص على أساس قناة صغيرة وكان عدد رينولد يتراوح بين 70 و 300 في معدل تدفق السوائل تراوحت من (4.6 لتر/ساعة إلى 18.35 لتر/ساعة) يستخدم للتحقيق التجريبي في درجة حرارة مدخل السائل (20°C درجة مئوية). كان السائل العامل البروبيلين جلايكول. يتم تقييم أداء قناة تجميع الطاقة الشمسية البسيطة من حيث معامل انتقال الحرارة، عدد نسلت، عامل الاحتكاك وضخ الطاقة. وتكشف النتيجة أنه عندما يكون هناك زيادة في معدل تدفق الكتلة من السائل المتدفق، فإن معامل انتقال الحرارة الحراري يزداد أيضا في حين ينخفض معامل الاحتكاك.

الكلمات المفتاحية: لوحة مسطحة، مصغرة- قناة، جامع الشمسية، معامل نقل الحرارة.